
This is an electronic reprint of the original article.
This reprint may differ from the original in pagination and typographic detail.

Mehrasa, Majid ; Sepehr, Amir; Pouresmaeil, Edris; Kyyrä, Jorma; Marzband, Mousa; Catalão, João P.S.

Stability Analysis of a Synchronous Generator-Based Control Technique used in Large-Scale Grid Integration of Renewable Energy

Published in:

Proceedings of the 2018 International Conference on Smart Energy Systems and Technologies (SEST)

DOI:

[10.1109/SEST.2018.8495888](https://doi.org/10.1109/SEST.2018.8495888)

Published: 01/01/2018

Document Version

Peer-reviewed accepted author manuscript, also known as Final accepted manuscript or Post-print

Please cite the original version:

Mehrasa, M., Sepehr, A., Pouresmaeil, E., Kyyrä, J., Marzband, M., & Catalão, J. P. S. (2018). Stability Analysis of a Synchronous Generator-Based Control Technique used in Large-Scale Grid Integration of Renewable Energy. In *Proceedings of the 2018 International Conference on Smart Energy Systems and Technologies (SEST)* IEEE. <https://doi.org/10.1109/SEST.2018.8495888>

This material is protected by copyright and other intellectual property rights, and duplication or sale of all or part of any of the repository collections is not permitted, except that material may be duplicated by you for your research use or educational purposes in electronic or print form. You must obtain permission for any other use. Electronic or print copies may not be offered, whether for sale or otherwise to anyone who is not an authorised user.

Stability Analysis of a Synchronous Generator-Based Control Technique used in Large-Scale Grid Integration of Renewable Energy

Majid Mehrasa Amir Sepehr, Edris Pouresmaeil,
C-MAST/UBI Jorma Kyyrä
Portugal Dep. of Elec. Eng. and Auto.,
Aalto University,
Finland

Mousa Marzband
Dep. of Mech. and Elec.
Eng. Northumbria
University,
UK

João P. S. Catalão
INESC TEC and FEUP, Porto,
C-MAST/UBI, Covilha, and
INESC-ID/IST-UL, Lisbon,
Portugal

Abstract—A synchronous generator (SG)-based control technique is proposed in this paper to force the grid voltage magnitude and frequency to follow the desired values under high penetration of renewable energy sources. The active and reactive power error-based curve of the proposed control technique is evaluated in detail. Besides, the grid angular frequency error based on the proposed control technique performance is assessed in the next step. Simulation is employed in Matlab/Simulink to verify operation of the proposed control technique in power converters for large-scale integration of renewable energy sources into the power grids.

Keywords—Renewables integration, double synchronous controller, power grid stability, virtual inertia, mechanical power.

I. INTRODUCTION

Integrating the large-scale renewable energy resources (RERs) into the power grid offers several benefits i.e., economic and environmental benefits [1]-[2].

In the meantime, it also increases different technical challenges regarding the grid stability and reliability due to the high variability, unpredictable fluctuation and intermittent characteristics of these sources [3]. Generally, RERs are connected to the power grid via power electronics converters [4], which the lack of inertia in these converter-based power generators, besides their peculiar transient dynamics behavior, increase their negative impacts on the power grid stability, just the opposite of the operation of synchronous generators.

Consequently, the operation of converter-based generators should be controlled with some specific functionalities based on inherent characteristics of synchronous generators; thus, successfully reaching their high penetration level in power grid [5]. Therefore, designing an appropriate control technique for grid-interfaced converters to deal with the stability issues of the power grid has been regarded as one of the main tasks for scientists in power and energy societies [6]-[7].

Various control aims such as accurate power sharing and grid voltage regulation have been considered in a large-scale integration of microgrid or multi-distributed generations (DG) connections for achieving a stable performance [8]-[9].

In addition, along with increasing the challenges of high penetration of RERs into the power grid [10]-[11], several control strategies have focused on improving the stability of grid frequency and voltage magnitude.

For this reason, several studies have been reported in the literature regarding the emulation of synchronous generator characteristics by power converters [12]- [16].

Reference [12] has presented a complete review associated with the main concepts of virtual synchronous generators and their ability at controlling the power grid under the high level of DGs penetration. A coordinated control-based energy storage system combined with virtual synchronous generators has been proposed in [13] to provide emulation of the synchronous generator for power converters. In [14], using a non-ideal proportional-resonant (PR) controller and SG features embedded in swing equation, a synchronous active proportional resonant-based control strategy has been proposed to control a grid-interfaced converter for high penetration of RERs into the power grid. Numerical simulations have been used in [15] to illustrate a specific virtual synchronous machine-based concept along with its related mathematical for controlling power converters in smart grid application. Reference [16] has proposed a power-based control technique to force the interfaced power converter to have the inherent features of synchronous power generators by injecting both active and reactive power into the power grid.

This paper presents a new control strategy based on synchronous generator features that provides a stable operating condition for the grid under high penetration of renewable energy resources. Then, a comprehensive stability analysis based on the active and reactive power error curve is presented. The grid angular frequency variations are also assessed. Simulation results show the ability of the proposed control technique for grid-interfaced converters to guarantee the stability of the power grid under high penetration of renewable energy sources.

II. THE PROPOSED CONTROL TECHNIQUE

The operating conditions of the power grid can be modeled by achieving the mathematical description of the interfaced converter. Considering the interfaced converter in Fig. 1, the dynamic model of the interfaced converter based on the d-q components of its currents can be driven as given in Eq. (1).

J.P.S. Catalão acknowledges the support by FEDER funds through COMPETE 2020 and by Portuguese funds through FCT, under Projects SAICT-PAC/0004/2015 - POCI-01-0145-FEDER-016434, POCI-01-0145-FEDER-006961, UID/EEA/50014/2013, UID/CEC/50021/2013, UID/EMS/00151/2013, and 02/SAICT/2017 - POCI-01-0145-FEDER-029803, and also funding from the EU 7th Framework Programme FP7/2007-2013 under GA no. 309048.

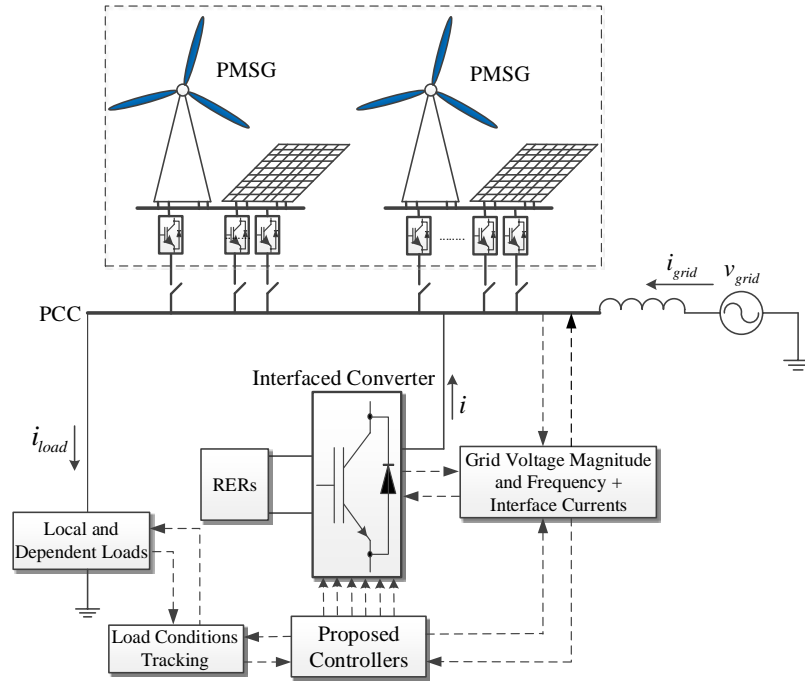


Fig. 1. General model for integration of large-scale RERs.

$$\frac{d}{dt} \begin{bmatrix} Li_d \\ Li_q \\ Cv_{dc} \end{bmatrix} = \begin{bmatrix} -R & \omega L & u_d \\ -\omega L & -R & u_q \\ -u_d & -u_q & 0 \end{bmatrix} \begin{bmatrix} i_d \\ i_q \\ v_{dc} \end{bmatrix} + \begin{bmatrix} -v_d \\ -v_q \\ -i_{dc} \end{bmatrix} \quad (1)$$

where L , R , ω are the inductance, resistance, and angular frequency of the interfaced converter, respectively. i_{dq} , v_{dq} and u_{dq} are the output currents, output voltages, and switching state functions of the interfaced converter in d-q reference frame, respectively. v_{dc} , i_{dc} and C are the dc-link voltage, dc-link current, and the capacitance of dc-link voltage, respectively. By assuming the converter active and reactive power as $P=i_d v_d$ and $Q=-i_q v_d$, (1) can be rewritten as:

$$\frac{d}{dt} \begin{bmatrix} \frac{L}{R} P \\ \frac{L}{R} Q \\ RCP_{c1} \end{bmatrix} = \begin{bmatrix} -1 & -\frac{\omega L}{R} & u_d \\ \frac{\omega L}{R} & -1 & -u_q \\ -u_d & u_q & 0 \end{bmatrix} \begin{bmatrix} P \\ Q \\ P_{c1} \end{bmatrix} + \begin{bmatrix} -P_{pd} \\ P_{pdq} \\ -P_{c2} \end{bmatrix} \quad (2)$$

where, $P_{c1}=v_{dc}v_d/R$, $P_{c2}=i_{dc}v_d$, $P_{pd}=v_d^2/R$, and $P_{pdq}=v_d v_q/R$. By transforming (2) into the frequency domain, (3) can be achieved as:

$$\begin{bmatrix} \frac{L}{R}(\frac{1}{s}+1) & \frac{\omega L}{R} & -u_d \\ -\frac{\omega L}{R} & \frac{L}{R}(\frac{1}{s}+1) & u_q \\ u_d & -u_q & RCs \end{bmatrix} \begin{bmatrix} P \\ Q \\ P_{c1} \end{bmatrix} + \begin{bmatrix} P_{pd} \\ -P_{pdq} \\ P_{c2} \end{bmatrix} = 0 \quad (3)$$

The relation between the electrical and mechanical parts of a synchronous generator can be stated by the following swing equation as:

$$J \frac{d\omega}{dt} = \frac{P_m - P}{\omega} \quad (4)$$

where J and P_m are the moment inertia and mechanical power of synchronous generator, respectively. By applying the small signal linearization to (4), the error of angular frequency can be calculated as:

$$\Delta\omega = \frac{1}{\omega^* J} \cdot \frac{\Delta P_m - \Delta P}{s + (P_m^* - P^*) / \omega^{*2} J} \quad (5)$$

where P_m^* , P^* , and ω^* are the reference values of active power, mechanical power, and angular frequency, respectively. By a control-based description of the active power error, the following equation can be achieved as:

$$\frac{\Delta P}{s} = \frac{\Delta P_m}{s} - \left(\omega^* J + \frac{(P_m^* - P^*)}{\omega^* s} \right) \Delta\omega \quad (6)$$

Assuming a constant power for the interfaced converter and using small signal linearization, gives:

$$\frac{\Delta Q}{s} = -\frac{P^*}{Q^*} \frac{\Delta P_m}{s} + \frac{P^*}{Q^*} \left(\omega^* J + \frac{(P_m^* - P^*)}{\omega^* s} \right) \Delta\omega \quad (7)$$

where Q^* is the reference value of reactive power. Using (5)-(7), the dynamic model of the interfaced converter based on characteristics of SG is given as:

$$\frac{1}{s} \begin{bmatrix} \Delta\omega \\ \Delta P \\ \Delta Q \end{bmatrix} = \begin{bmatrix} 0 & \frac{-1/\omega^* J s}{s + (P_m^* - P^*) / \omega^{*2} J} & 0 \\ -\left(\omega^* J + \frac{(P_m^* - P^*)}{\omega^* s} \right) & 0 & 0 \\ \frac{P^*}{Q^*} \left(\omega^* J + \frac{(P_m^* - P^*)}{\omega^* s} \right) & 0 & 0 \end{bmatrix} \begin{bmatrix} \Delta\omega \\ \Delta P \\ \Delta Q \end{bmatrix} + \begin{bmatrix} \frac{1}{\omega^* J s} \cdot \frac{1}{s + (P_m^* - P^*) / \omega^{*2} J} \\ \frac{1}{s} \\ -\frac{P^*}{Q^*} \frac{1}{s} \end{bmatrix} \Delta P_m \quad (8)$$

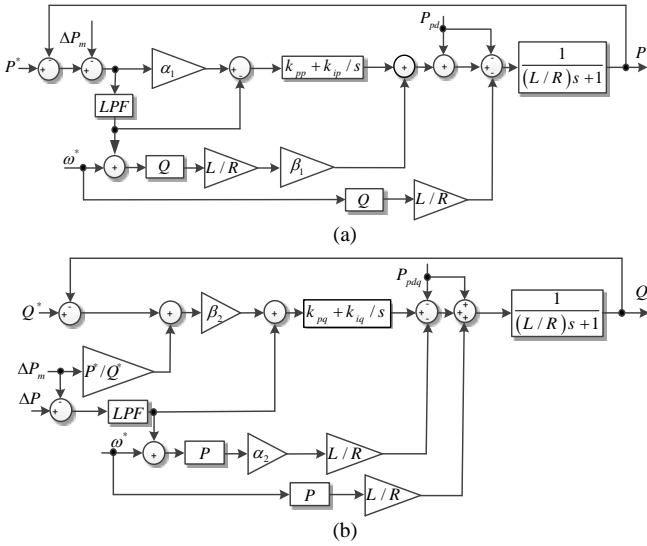


Fig. 2. The proposed control technique based on inherit feature of synchronous generator.

III. EVALUATION OF THE ACTIVE AND REACTIVE POWER ERROR-BASED CURVE

By applying small-signal linearization to two first terms of (2), equations (9) and (10) can be achieved as:

$$\frac{L}{R}s\Delta P + \Delta P + \frac{\Delta\omega L}{R}Q^* + \frac{\omega^* L}{R}\Delta Q - \Delta u_d P_{c1}^* - u_d^* \Delta P_{c1} + \Delta P_d = 0 \quad (9)$$

$$\frac{L}{R}s\Delta Q + \Delta Q - \frac{\Delta\omega L}{R}P^* - \frac{\omega^* L}{R}\Delta P + \Delta u_q P_{c1}^* + u_q^* \Delta P_{c1} - \Delta P_{dq} = 0 \quad (10)$$

where u_{dq}^* and P_{c1}^* are the reference values of switching functions and P_{c1} , respectively. And also combining (6), (7), (9) and (10), the error curve for the DSC's active and reactive power can be achieved as (11):

$$(\Delta P + a_{DSC})^2 + (\Delta Q + b_{DSC})^2 = R_{DSC}^2 \quad (11)$$

where $(-a_{DSC}, -b_{DSC})$ and R_{DSC} are the radius and center parameters, respectively. The radius and center parameters of the active and reactive power error curve are specified as:

$$R_{DSC} = \sqrt{\left(\frac{(P_m^* - P^*)LQ^*\Delta\omega - \omega^*LQ^*\Delta P_m - R\omega^{*2}J\Delta\omega Q^* - \omega^{*3}JP^*L\Delta\omega}{2\omega^*LQ^*} \right)^2 + \left(\frac{L\omega^*P^*\Delta P_m - \omega^{*3}J\Delta\omega LQ^* - LP^*(P_m^* - P^*)\Delta\omega + \omega^{*2}JP^*R\Delta\omega}{2LQ^*\omega^*} \right)^2} + \frac{\left(\begin{aligned} &\omega^*JLQ^{*2}\Delta\omega^2 - \omega^*JP_{c1}^*Q^*R\Delta u_d\Delta\omega - \omega^*JQ^*Ru_d^*\Delta P_{c1}\Delta\omega \\ &+ \omega^*JQ^*R\Delta P_d\Delta\omega + \omega^*JP^*L\Delta\omega^2 \\ &- \omega^*JP^*RP_{c1}^*\Delta u_q\Delta\omega - \omega^*JP^*Ru_q^*\Delta P_{c1}\Delta\omega + \omega^*JP^*R\Delta P_{dq}\Delta\omega \end{aligned} \right)}{Q^*L}$$

$$a_{DSC} = \left(\frac{(P_m^* - P^*)LQ^*\Delta\omega - \omega^*LQ^*\Delta P_m - R\omega^{*2}J\Delta\omega Q^* - \omega^{*3}JP^*L\Delta\omega}{2\omega^*LQ^*} \right)$$

$$b_{DSC} = \left(\frac{L\omega^*P^*\Delta P_m - \omega^{*3}J\Delta\omega LQ^* - LP^*(P_m^* - P^*)\Delta\omega + \omega^{*2}JP^*R\Delta\omega}{2LQ^*\omega^*} \right)$$

The virtual mechanical power error alterations can impact on the active and reactive power error curve of the proposed control-based interfaced converter according to Fig. 3.

As it is expected, increasing virtual mechanical power error leads to the larger error curve, which shows the importance of virtual control technique.

Choosing different values for the virtual inertia can cause the error curve to be changed based on Fig. 4. According to this figure, the critical case is associated with very high value of the virtual inertia that generates the largest error curve.

For the low-high values of the virtual inertia, the best response is achieved. But, selecting very low values for the virtual inertia can lead to larger curve but not as the same that is obtained for very high virtual inertia, as illustrated in Fig. 4. It can be understood from Fig. 4, the virtual inertia of the proposed synchronous generator-based control strategy plays a key role at reaching the decreased values for both active and reactive power errors.

IV. ASSESSMENT OF THE GRID FREQUENCY VARIATIONS

The small signal method is applied to the first term of (2) and subsequently (12) can be obtained as:

$$\left(\frac{L}{R}s + 1 \right) \Delta P + \frac{\Delta\omega L}{R}Q^* + \frac{\omega^* L}{R}\Delta Q \quad (12)$$

$$-\Delta u_d P_{c1}^* - u_d^* \Delta P_{c1} + \Delta P_d = 0$$

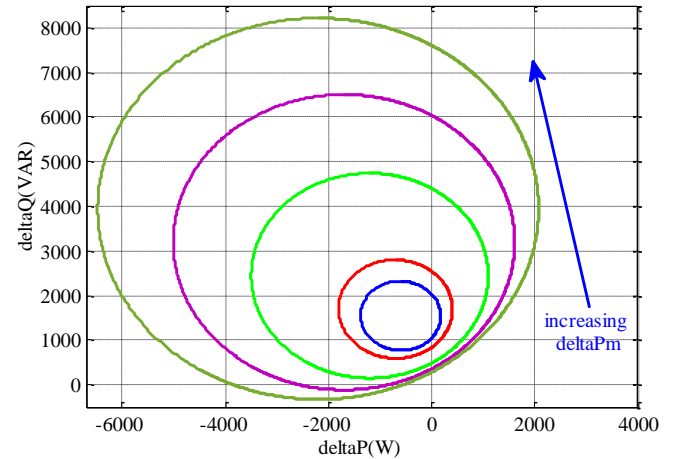


Fig.3. The effects of increasing ΔP_m on the DSC error curve.

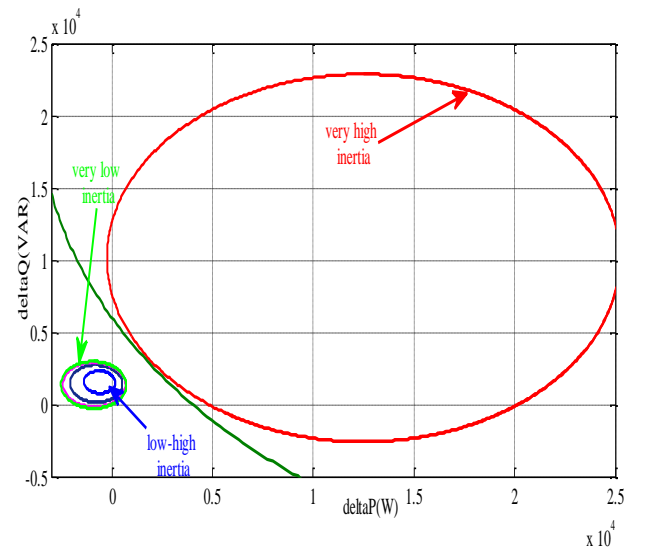


Fig. 4. The effects of changing the virtual inertia (J) on the DSC error curve.

By achieving ΔP from (6) and substituting the result into (12), variations of the grid frequency can be achieved as:

$$\Delta\omega = F_{P_m} \Delta P_m + F_Q \Delta Q + F_{u_d} \Delta u_d + F_{P_{c1}} \Delta P_{c1} + F_{P_d} \Delta P_d \quad (13)$$

$$F_{P_m} = \frac{\left(\frac{L}{R}s + 1\right)}{\Delta\omega}, F_Q = \frac{\omega^* L}{\Delta\omega}, F_{u_d} = -\frac{P_{c1}^*}{\Delta\omega},$$

$$F_{P_{c1}} = -\frac{u_d^*}{\Delta\omega}, F_{P_d} = \frac{1}{\Delta\omega} \quad (14)$$

$$\Delta\omega = \left(\frac{\omega^* J L}{R} s^2 + \left[\left(\frac{(P_m^* - P^*) L}{R \omega^*} \right) + \omega^* J \right] s + \left[(P_m^* - P^*) / \omega^* + \frac{Q^* L}{R} \right] \right)$$

Based on (13), the effects of each component are considered to evaluate the responses of the grid angular frequency versus the varied values of virtual inertia. As can be seen from (13) and (14), the transfer function relating to the virtual mechanical power error is different from other components errors. For three virtual inertia values of $J_3 > J_2 > J_1$, the Nyquist diagrams of transfer functions around the operating angular frequency associated with the virtual mechanical power error and other errors are drawn in Fig. 5. Based on Figs. 5(a) and (b), it can be explained that increasing the virtual inertia leads to better response for the grid angular frequency error under the presence of various error components. In fact, increasing the virtual inertia can help the proposed controller to reach a grid frequency near to its reference value with almost zero error.

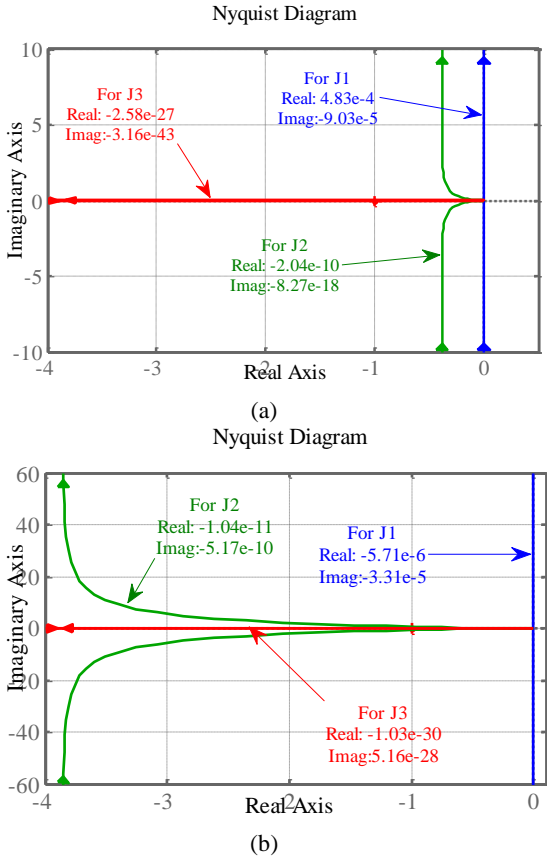


Fig. 5. The Nyquist diagram of $\Delta\omega$ versus the step variation of: (a) VMPE (ΔP_m), and (b) other components errors (ΔQ , Δu_d , ΔP_{c1} , and ΔP_d).

V. RESULTS AND DISCUSSIONS

In this section, the ability of the synchronous generator-based control technique is assessed based on regulating the grid frequency and voltage magnitude at their desired values. The simulations are performed in MATLAB/SIMULINK software and the system parameters are given in Table I.

A. Grid frequency and voltage magnitude evaluation

The operation of the proposed control technique can be affected by various values of the virtual inertia. To deal with power grid stability through performance of the proposed control strategy, the acceptable region of the inertia values is assessed in this sub-section.

A divergence behavior for both grid frequency values due to very low and high inertia can be seen in Fig. 6(a) in which the divergence rate for very high inertia is much more than another one. On the other hand, the grid voltage magnitude due to very low inertia can hardly move on the upper path of its desired value with high fluctuations. But, choosing a very high value of the inertia leads to an uncontrollable behavior from the grid voltage magnitude with severe fluctuations as depicted in Fig. 6(b).

TABLE I: SIMULATION PARAMETERS

Parameter	Value	Parameter	Value
dc-link Voltage (v_{dc})	850 V	J	1e3 s
Phase ac voltage	220 V	P_m	3.3 kW
Fundamental frequency	50 Hz	P	3 kW
Switching frequency	10 kHz	Q	2 kVAr
Interface converter resistance	0.1 Ohm	Interface converter inductance	45 mH

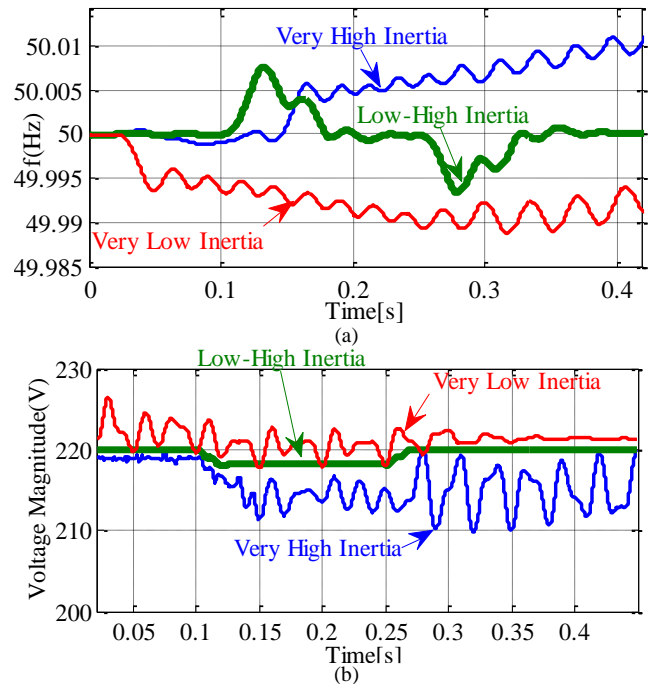


Fig. 6. Various values of inertia on the proposed control technique: (a) grid frequency, and (b) grid voltage magnitude.

VI. CONCLUSION

A control technique based on inherent features of synchronous generators as well as the power-based dynamic model of interfaced converters has been introduced in this paper. All effects of the virtual inertia and mechanical power error upon the active and reactive power error have been assessed completely by the use of a power error-based curve. Moreover, the grid angular frequency alterations have been investigated. The operation of the proposed control technique has been evaluated by simulation results through the Matlab/Simulink. The obtained results confirmed the accurate performance of the proposed control technique for grid-interfaced converters to guarantee a stable operating condition for the power grid under high penetration of renewable energy sources.

REFERENCES

- [1] H. Lund and B. V. Mathiesen, "Energy system analysis of 100% renewable energy systems—The case of Denmark in years 2030 and 2050," *Energy*, vol. 34, no. 5, pp. 524–531, May 2009.
- [2] E. Pouresmaeil, H.R. Shaker, M. Mehrasa, M.A. Shokridehaki, E.M.G. Rodrigues, and J.P.S. Catalão, "Integration of renewable energy for the harmonic current and reactive power compensation," *POWERENG*, Sep. 2015.
- [3] M. Mehrasa, E. Pouresmaeil, B.N. Jørgensen, and J.P.S. Catalão, "A control plan for the stable operation of microgrids during grid-connected and islanded modes," *Electric Power Systems Research*, vol. 129, pp. 10-22, Dec. 2015.
- [4] A. Trivedi, M. Singh, "Repetitive Controller for VSIs in Droop-Based AC-Microgrid," *IEEE Transactions on Power Electronics* 2017; 32 (8): 6595 – 6604.
- [5] E. Pouresmaeil, H. R. Shaker, M. Mehrasa, M.A. Shokridehaki, E. M.G. Rodrigues, J.P.S. Catalão, "Stability analysis for operation of DG units in smart grids," *POWERENG*, Sep. 2015.
- [6] V. Nasirian, Q. Shafiee, JM. Guerrero, FL. Lewis, A. Davoudi, "Droop-Free Distributed Control for AC Microgrids," *IEEE Transactions on Power Electronics* 2016; 31 (2): 1600 – 1617.
- [7] M. Mehrasa, M. Rezanejad, E. Pouresmaeil, J.P.S. Catalão, S. Zabihi, "Analysis and control of single-phase converters for integration of small-scaled renewable energy sources into the power grid," *7th Power Electronics and Drive Systems Technologies Conference (PEDSTC)*, 384-389, Sep. 2016.
- [8] V. Karapanos, P. Kotsampopoulos, N. Hatzigiorgiou, "Performance of the linear and binary algorithm of virtual synchronous generators for the emulation of rotational inertia," *Electric Power Systems Research* 2015; 123: 119-127.
- [9] L. Yang, J. Wang, Y. Ma, J. Wang, X. Zhang, LM. Tolbert, FF. Wang, K. Tomsovic, "Three-Phase Power Converter-Based Real-Time Synchronous Generator Emulation," *IEEE Transactions on Power Electronics* 2017; 32 (2): 1651 – 1665.
- [10] P.M.R. Almeida, F.J. Soares, J.A.P. Lopes, "Electric vehicles contribution for frequency control with inertial emulation," *Electric Power Systems Research* 2015; 127: 141-150.
- [11] M Guan, W Pan, J Zhang, Q Hao, J Cheng, X Zheng, "Synchronous Generator Emulation Control Strategy for Voltage Source Converter (VSC) Stations," *IEEE Transactions on Power Systems* 2015; 30 (6): 3093 – 3101.
- [12] H Bevrani, T Ise, Y Miura, "Virtual synchronous generators: A survey and new perspectives," *International Journal of Electrical Power & Energy Systems* 2014; 54: 244-254.
- [13] J Fang, Y Tang, H Li, X Li, "A Battery/Ultracapacitor Hybrid Energy Storage System for Implementing the Power Management of Virtual Synchronous Generators," *IEEE Transactions on Power Electronics* 2018; 33 (4); 2820 – 2824.
- [14] M. Mehrasa, R. Godina, E. Pouresmaeil, I. Vechiu, R. L. Rodríguez, J. P. S. Catalão, "Synchronous active proportional resonant-based control technique for high penetration of distributed generation units into power grids," *Innovative Smart Grid Technologies Conference Europe (ISGT-Europe)*, 2017 IEEE PES, pp. 1-6, January 2018.
- [15] S. D'Arco, JA. Suul, OB. Fosso, "A Virtual Synchronous Machine implementation for distributed control of power converters in Smart Grids," *Electric Power Systems Research* 2015; 122: 180-197.
- [16] E. Pouresmaeil, M. Mehrasa, R. Godina, I. Vechiu, R. L. Rodríguez, J.P.S. Catalão, "Double synchronous controller for integration of large-scale renewable energy sources into a low-inertia power grid," *Innovative Smart Grid Technologies Conference Europe (ISGT-Europe)*, 2017 IEEE PES, pp. 1-6, January 2018.